Study of biomolecules adsorption on carbon nanotubes for their application as biosensors

Final Master Project

Master Degree in Nanostructured Materials for Nanotechnology Applications

Author: Mónica González García

Directors: Dra. Mª Teresa Martínez Fernández de Landa

Dra. Pilar Cea Mingueza

INDEX

1. Introduction

The work presented in this dissertation has been carried out in the framework of the research line of the group Carbon Nanostructures and Nanotechnology (G-CNN), which belongs to the Instituto de Carboquímica (ICB) of the Spanish National Research Council (CSIC).

Biological sensing techniques are usually based on optical detection. Despite being very sensitive and specific, those techniques are quite complex, requiring multiple steps (sample purification, signal amplification), are difficult to miniaturize and have relatively high limits of detection.

Detection using nanoscale devices, mainly electronic devices, ideally allow detecting much lower quantities of analyte with fewer sample preparation. Field effect transistors (FETs) using a single-wall carbon nanotube (SWNT) as the conducting channel are well known and studied. As SWNTs have a very high specific surface area, they are very sensitive to environmental changes, and their electronic behavior can change with very small amounts of substances being adsorbed on their surface.

However, before using SWNTs in a FET sensor, specific and non specific adsorption of different species present in the sample must be taken into account. Their high sensitivity makes them also sensible to other substances present in the media, and false positive can be obtained when not careful studies of specific adsorption have been carried out.

The main goal of this work is to determine and control non-specific adsorption on the surface of the carbon nanotubes in order to use them as part of biosensors. Specific objectives of this work are the following:

- Production and functionalization of carbon nanotubes, and their characterization.
- Evaluation of biomolecule adsorption (streptavidin) on carbon nanotube surface.
- Linkage of DNA strand to the surface of the nanotubes to optically detect the hybridization with the complementary strand.

2. Revision of the state of the art

2.1. Carbon and its allotropic forms

The electronic configuration of carbon, $1s^2\ 2s^2 2p^2$, allows different hybridization possibilities. This leads to different coordination numbers, and thus to the existence of different allotropic structures. Diamond and graphite are the two crystalline forms of carbon that can be found in nature. Diamond present sp^3 hybridization and the atoms of carbon are organized in a tridimensional network. All the electrons are localized in the bonds. Diamond is really hard and rigid and behaves as an insulator. On the other hand, graphite is characterized by a sp^2 hybridization, with the carbon atoms forming a hexagonal planar network. Different sheets interact by π-interactions. Graphite is a soft anisotropic material, and behaves like a metal.

The third allotropic form of carbon was discovered in 1985: the fullerenes[1]. Fullerenes are closed carbon structures, showing spherical shape and a hollow interior. The most abundant one, and the most stable and symmetric, is C60. Some interesting properties, like superconductivity or ferromagnetism, have been found in fullerenes.

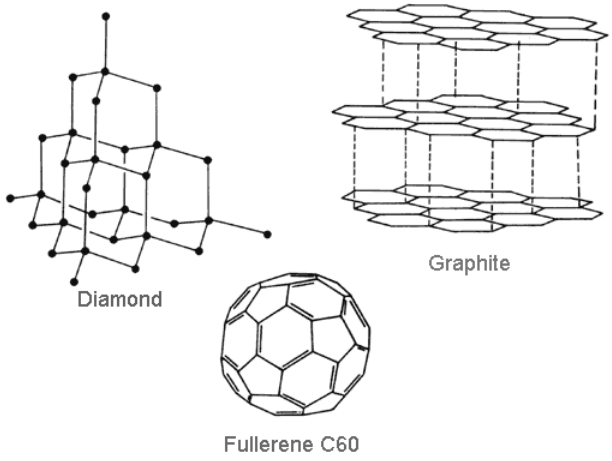

Figure 1: Atomic structure of diamond, graphite and fullerene C60.

In 1991, Ijima[2] discovered the fourth allotropic structure of carbon, the carbon nanotubes (CNTs). They can be considered as a rolled-up graphene sheet forming a tube. The end of the tube can be open, or closed by a semisphere with a structure similar to that of a fullerene.

Two main types of CNTs can be found depending on the number of walls. Single Walled Carbon Nanotubes (SWNTs), can be defined as a single rolled-up graphene

sheet (Figure 2A). They were first observed in 1993[3,4] and have diameters between 1 and 3 nm. They self-organize forming bundles comprising even hundreds of tubes.

Multi Walled Carbon Nanotubes, MWNTs, can be defined as several concentric rolled-up graphene sheets (Figure 2B), perfectly graphitized and closed at the ends by carbon atom pentagons. The number of walls building de MWNTs is variable. The inner diameter varies from 1 to 3 nm, and the outer diameter is usually between 2 and 25 nm, depending on the number of walls. The space between layers is around 3.4 Å, slightly higher than the value of graphite (3.35 Å). According to Iijima[2,5], this difference is due to a combination of the graphene sheet curvature and the weak Van der Waals forces between concentric tubes.

The length of both types of nanotubes can vary from tens of nanometers to several microns.

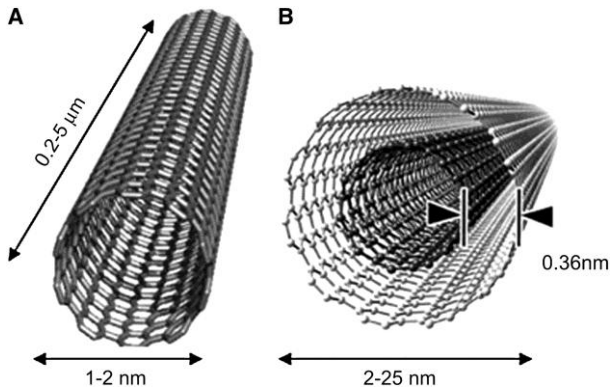

Figure 2: The two types of CNTs: A) SWCNT, B) MWNT.

2.2. Structure of carbon nanotubes

The carbon atoms forming the structure of CNTs have sp^2 hybridization. The different possible ways to roll a sheet of graphene to form a tube give rise to the different chiral or achiral dispositions.

Achiral configurations are known as armchair and zig-zag. In the armchair configuration, the C-C bonds of two opposite sides of the hexagon are perpendicular to the tube axis (Figure 3A). In the zig-zag configuration, those bonds are parallel to the tube axis (Figure 3B). The rest of possible configurations, where the C-C bonds form an angle θ respective to the tube axis, are known as chiral or helicoidal structures (Figure 3C).

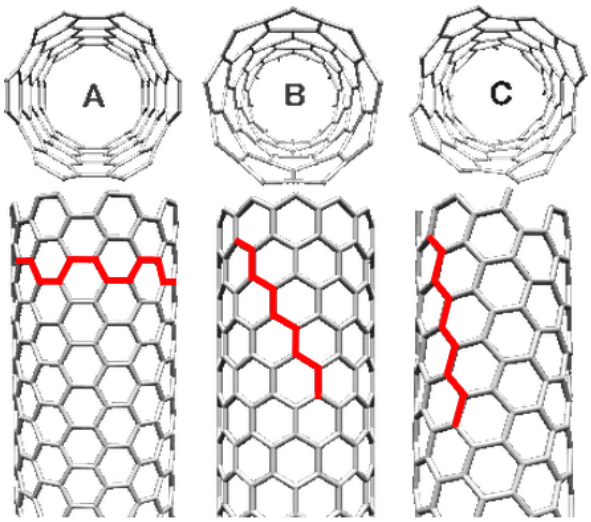

Figure 3: Molecular models showing different structures of SWNTs: A) armchair configuration, B) Zig-zag configuration, C) Chiral configuration.

Nanotubes chirality and electronic properties

The chirality of a tube can be defined in terms of the chiral vector, C_n ($C_n = na_1 + ma_2$), which also defines the tube diameter[6], *d*. This vector defines the rolling direction of the graphene sheet, with a point *(m,n)* superimposed over a defined origin (0,0) (Figure 4). The diameter of the tube can be expressed as:

$$d = \frac{a\sqrt{m^2 + mn + n^2}}{\pi} \qquad (1)$$

where $a = 1.42x\sqrt{3}$ Å corresponding to the constant distance in the graphene sheet. It must be taken into account that this distance is 1.42 Å for the sp^2 hybridization of carbon.

The chiral angle θ, the angle between the quiral vector and the rolling direction of the graphene sheet, is defined as

$$\theta = \arctan\left[-\frac{\sqrt{3}n}{2m+n}\right] \qquad (2)$$

For the zig-zag structure, θ = 0º, and the values *(n,m)* results in *(n, 0)* or *(0, m).*

For the armchair structure, θ = ±30º, and the values *(n,m)* results in *(n, n).*

The rest of values *(n,m)* stand for chiral structures.

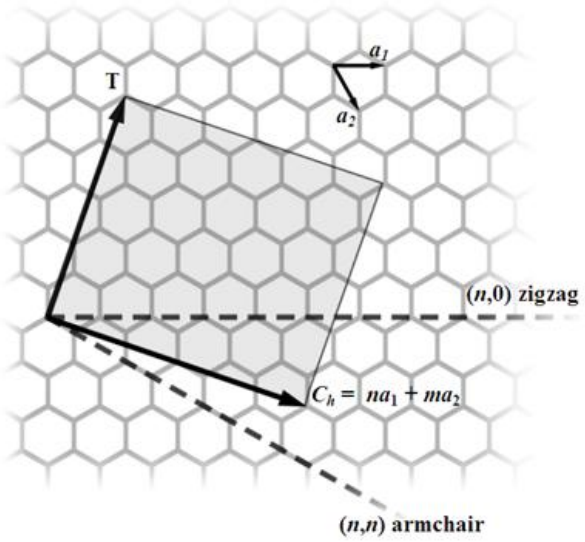

Figure 4: Chiral vector C_n defining the chirality of a carbon nanotube.

The conductive properties of carbon nanotubes are defined by the diameter and quiral angle. When the value of the term $2n+m$ is a multiple of 3, $2n+m=3q$ being q an integer, the nanotube is metallic[7]. According to this expression, one third of the SWNTs are metallic, and two thirds are semiconductive. This fact has been confirmed by conductance measurements with Atomic Force Microscope (AFM) over individual nanotubes[8].

2.3. Properties and applications

Concerning the exceptional properties of CNTs, a large Young modulus, high thermal conductivity, electronic transport and large length to diameter ratio can be highlighted. Since the CNTs used in this work are SWNTs, the following properties and applications are focused on that of SWNTs.

As their structure consists only of C atoms, SWNTs form a very light material, with a density of about 1.3 g/cm^3. As the C-C bond is one of the strongest chemical bonds, CNTs have high strength, although the defects present in their structure make the observed values for mechanical resistance and Young modulus lower than those expected from the calculated values. Values of Young modulus up to 1 TPa[9] have been found, hundredfold higher than that of steel. It has been also proved that they are a very flexible material, withstanding being bent big angles without breaking[10]. However, the values obtained vary depending on the measuring technique.

Isolated SWNTs show this property[9], but when bundles of SWNTs are considered, it has been proved that the mechanical resistance is not so high, due to the tubes sliding over one another and/or to the presence of structural defects[11].

Due to the high thermal conductivity SWNTs show along their axis, values up to 3500 W/m·K[12] are found. Thus, SWNTs are one of the best thermal conductors known (copper has a conductivity of 385 W/m·K), making them suitable for applications where heat dissipation is an important factor, including electronic, computer and space applications.

The quasi-unidimensional structure of CNTs together with the periodicity of the disposition of the carbon atoms along the axis provides them with unusual electronic properties. These properties are related to their structure, and so depend both on the diameter and on the chirality of the tube, as explained before. The electronic transport along the nanotube is ballistic, giving rise to a high current density conduction of electrons along the axis[13].

As a consequence of their electronic and mechanical properties, the CNTs are suitable for applications in nanoelectronics, aeronautics, automotive, and as reinforcement materials for nanocomposites, among other applications.

In addition, if their high specific surface area is considered together with their high electrical conductivity, and the capacity to behave both as electron donor or acceptor, they are excellent candidates for electrochemical applications and chemical sensors.

A more general revision of the applications of carbon nanotubes can be found in reference 14.

2.4. Carbon nanotubes and biosensors

The use of CNTs in biochemistry has been limited by their insolubility in aqueous solvents. However, they are suitable for non invasive and high sensitive detection, since they have near-infrared intrinsic fluorescence, Raman resonance and photoacoustic signal related to the graphene structure in SWNTs. This is the reason why they are being studied for different biomedical applications[15].

Several ways of making them soluble have been tried, including covalent functionalization[16-20] and non-covalent interaction with polymers[21-23], surfactants and other amphiphilic molecules[24,25] , DNA[26] and amines[27].

Their unique properties and the fact that their functionalization and debundling make them non-toxic[28,29] , has stimulated increasing interest in the use of CNTs as components in bioapplications, such as biosensors and intracellular transporters[30-33]. In order to use them in biosensors, biological species as enzymes[34] and proteins[35-37] have been immobilized either in the hollow cavity[38] or on the surface of the nanotube. In that context, the control of non-specific protein adsorption is important for the use of CNTs in specific protein-binding or bio recognition[39]. Several examples have been proved to work properly with academic samples, when pure components are used, but they have given false positives when using real samples. If we consider only proteins, more than 250 different ones are present in human plasma[40] and more than 450 in human blood serum[41], in a range of 10 orders of magnitude in concentration. The non-specific adsorption of any of these proteins is very difficult or even impossible to distinguish from the binding of the desired target[42].

There are several molecules reported in the literature that have been used to prevent the protein adsorption. PEG forms highly inert coatings that can resist adsorption of a variety of proteins[43]. PEG is a water-soluble polymer capable of extensive hydrogen bonding that swells in aqueous solutions and satisfies all the properties for surface coatings that greatly resist non-specific protein adsorption, as outlined by Ostuni et al.[44] PEG, bonded no covalently to CNTs has been used to achieve the protein resistance, with different results[39]. Dai et al.[37] reported that the coverage of SWNTs, grown on SiO_2 substrate, was not complete or uniform with PEG, finding some streptavidin adsorption on them. Nevertheless, these authors have reported that the co-adsorption of Triton and PEG on SWNTs was highly effective in preventing nonspecific adsorption of streptavidin on nanotubes. Chen et al.[45] adsorbed Tween®20 and Pluronic® P103, both containing PEG units, on as-grown SWNTs on quartz substrates. These authors found that the modified SWNTs were resistant towards proteins such as streptavidin, avidin, bovine serum albumin, α-glucosidase and staphylococcal protein A.

The protein resistant coating usually requires amphiphilic molecules with a hydrophobic backbone that interacts hydrophobically with the CNT and a hydrophilic segment extended in the aqueous solution. Surfactants molecules, that form non specific interactions with the nanotubes, have been also used to avoid non specific adsorption of biomolecules on CNTs[46]. The length and shape of the alkyl chain is very important for the efficiency of the interactions[47,48]. Compared to common surfactants, polymers usually have stronger surface adsorption due to the presence of more interaction sites and they could provide a suitable wrapping of CNTs.

The extremely high affinity of streptavidin and biotin, with a dissociation constant on the order of 10^{-14} mol/L, make it one of the strongest non covalent interaction known in nature. Streptavidin is a 60 KDa tetrameric protein obtained from *Streptomyces avidinii*. Biotin is a water soluble B-complex vitamin. This specific interaction has been widely used in biochemistry, and has also been used to link biomolecules to SWNTs.

Erdem et al.[49] fabricated disposable graphite pencil electrodes modified with MWNTs-streptavidin conjugates, and were used to electrochemically monitor label-free DNA hybridization. The biosensor built was able to differentiate complementary sequences from non complementary ones, and to select the target sequence DNA from a mixture with high sensitivity.

Liu et al.[50] prepared SWNT-streptavidin complexes via biotin-streptavidin recognition. They were able to attach biotinylated DNA, fluorophores and Au nanoparticles to the surface of SWNT-complexes. The complexes were stable for 18 days, showing high loading capacity.

Gao et al.[51] have used another strategy to electrochemically detect DNA down to the attomolar level. A molecular beacon (MB) is a single-strand hybridization probe, with a stem-loop structure. The MB, functionalized with biotin and thiol at 5' and 3' respectively, was immobilized on the surface of a carbon electrode modified with gold nanoparticles and 1-pyrenebutyrate functionalized graphene. In absence of the target DNA strand, the MB was in the "closed" state, where the biotin end was not accessible due to steric hindrance. After hybridization with target DNA, the loop was opened, and the biotin end was "open", and accessible to the detection probe.

MWNTs covalently functionalized with streptavidin-HRP (horse radish peroxidase) were used as detection probe, as the nanotubes accelerate the electron-transfer of the enzymatic catalytic reaction of HRP. Differential pulse voltammetric (DPV) measurement of the reaction was performed to detect the target DNA hybridization.

Carbon nanotubes and Field Effect Transistors

Field effect transistors have been used from 1960[52]. Field effect transistors (FETs) are a family of transistors that uses an electric field to control the conductivity of a channel in a semiconductor material. They can be considered as resistances controlled by a potential difference.

FETs are composed by three terminals. Source terminal (S), through which the majority charge carriers (electrons or holes) enter the channel. Drain terminal (D), through which the majority of charge carriers leave the channel. These two terminal conductors are connected to a semiconductor through ohmic contacts. The conductivity of the channel is a function of the potential applied to the third terminal, the gate terminal (G). It modulates the channel conductivity, allowing or blocking the electrons flow through the channel created between source and drain. By applying voltage to G, the current leaving the channel at D (I_D) can be controlled. Drain to Source voltage is called V_{DS}. The substrate or base can be considered as a fourth terminal. It is a semiconductor material where the other three terminals are comprised.

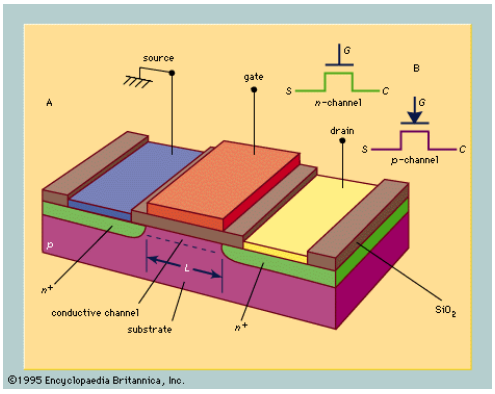

Figure 5. (A) Perspective of a MOSFET with (B) symbols for *n*- and *p*-channel devices. (Reference 53)

The possibility of using SWNTs as part of FETs was first stablished in 1998[54,55]. Both single carbon nanotube and carbon nanotubes networks have been used as conducting channels. The electric conductance of a CNT is extremely sensitive to its

environment and it can vary significantly with the surface interaction with chemical or biological species. This behavior has promoted the development of miniaturized sensors based on SWNTs as part of Field Effect Transistors (FETs) for the detection on biological molecules[56-57]. Sensors based on FETs are easier to miniaturize than ELISA (enzyme-linked inmunosorbent assay) or PCR (polymerase chain reaction) tests; require short measurement times and several samples can be measured at the same time. Studies about the interaction of CNTs with proteins in solution[35-38], enzymes[32,34] or peptides[58] have been developed. The nanotube density has also been studied, as a parameter influencing the performance of biosensors using CNT-FETs[59].

The successful use of SWNTs in FETs for electronic anabolic steroid recognition[60] and label-free DNA detection[61] has already been probed by our research group.

3. Experimental Section

3.1. Carbon nanotubes synthesis and functionalization

Single-walled nanotubes were produced by arc discharge method. A homemade reactor was used (Figure 6).

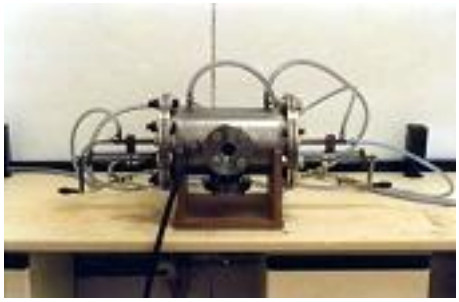

Figure 6: Arc discharge reactor used for the synthesis of SWNTs.

A rod of graphite was used as cathode. The anode was a graphite rod in which a hole had been drilled and filled with a mixture of graphite powder and metallic catalysts. Ni and Y were used as catalysers, in a molar ratio of 2:0.5. The arc discharge was created by applying a current of 100A, 20V, between the electrodes under 660mb of helium[62.63]. A constant distance (around 5 mm) was maintained between the electrodes.

Most of the material was condensed on the refrigerated walls, and web-like structures were deposited between the cathode and the reactor walls. The material was recovered after several rods burning.

The as-produced SWNTs were a multicomponent material consisting of entangled SWNT bundles associated with metal nanoparticles and carbon phases more or less graphitized (Figure 7).

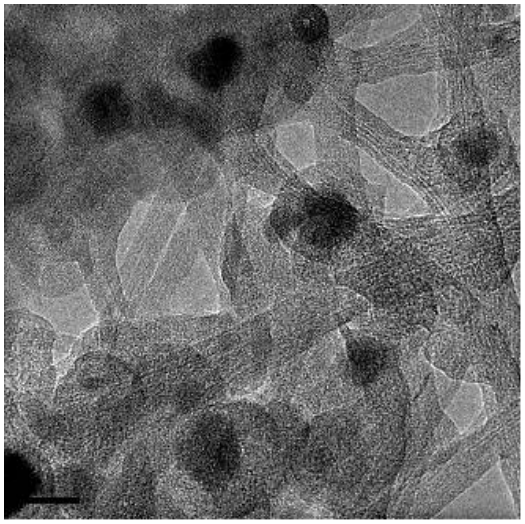

Figure 7: TEM image of as-produced SWNTs.

3.1.1. SWNTs covalent functionalization[64-66]

Different groups were introduced on the surface of the SWNTs in order to evaluate the influence of the different groups and charges on the streptavidin absorbance.

As grown SWNTs have some functional groups, but in a small number. Their surface can be considered as non charged. To obtain negative charge on the surface of the SWNTs, carboxylic groups ($COOH/COO^-$) were introduced. Amine groups (NH_2/NH_3^+) were produced in order to have positive surface charges. SWNTs were functionalized with biotin groups to have the most favourable conditions for streptavidin interaction.

The SWNTs have been intended to be blocked by covalently attaching polyethylene glycol (PEG) to their surface. This way, the streptavidin interaction with the SWNTs surface intends to be prevented.

Primary functionalization of SWNTs was carried out by oxidation in acid medium. 150 mg of as-grown SWNTs were added to 60 mL of an aqueous solution of nitric acid 1.5M and refluxed for 2 hours. The resulting suspension was then centrifuged during 4 hours at 10000 rpm, filtered through a 3 μm pore size Isopore filter, washed with milli-Q water until neutral pH was reached, and dried under vacuum. Besides the introduction of oxygenated groups, a reduction of the metal content was achieved.

To obtain aminated SWNTs, acid treated carbon nanotubes were first acylated. 40 mL of thionyl chloride and 2 mL of dimethylformamide were added to 200 mg of acid treated SWNTs, and stirred at 120ºC during 24 hours. After filtration through a 200 nm pore size PTFE membrane and washing with tetrahydrofuran to remove the $SOCl_2$ excess, the SWNT material was dried under vacuum. Afterwards, SWNTs material was mixed with 15 mL of ethylenediamine and stirred at 60ºC during 4 days. SWNTs dispersion was then filtered through a 200 nm PTFE membrane filter, washed repeatedly with ethanol and dried under vacuum to obtain the final aminated nanotubes.

The aminated nanotubes (60 mg) were then dispersed in dimethylformamide, and reacted overnight with N-hydroxysuccinimidyl biotin (120 mg) at room temperature

to form biotinated SWNTs. The dispersion was then filtered, rinsed and dried under vacuum.

A scheme of the sequence of reactions is shown in Scheme 1.

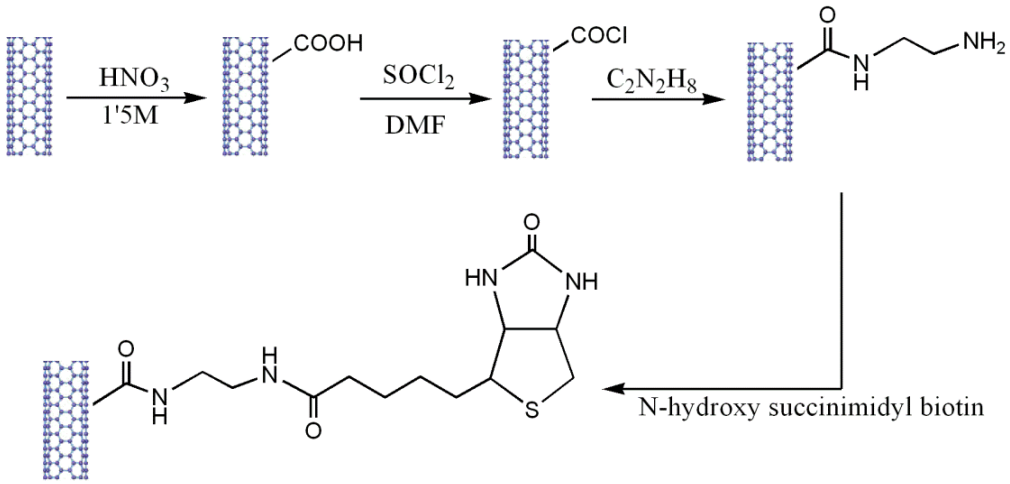

Scheme 1: Scheme of biotin functionalization of SWNTs.

To obtain SWNTs covalently functionalized with polyethylene glycol (Scheme 2), the acylated nanotubes were mixed with PEG and 2 mL of pyridine in 200 mL of dimethylformamide, and stirred at 100ºC during 5 days. After filtration, the product was washed with water and dried under vacuum.

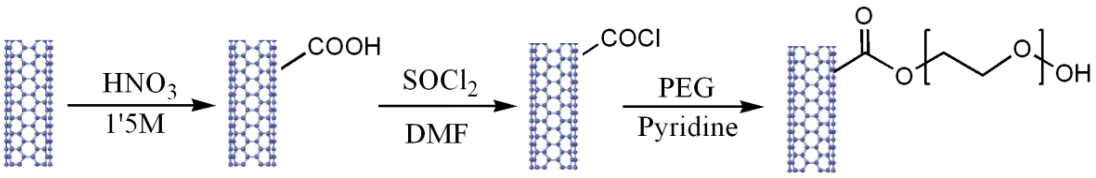

Scheme 2: Scheme of PEG covalent functionalization of SWNTs.

3.1.2. SWNTs non-covalent functionalization

The non-covalent functionalization has been carried out with PEG (average MW≈10000), Tween 20® and Pluronic F-127® (all of them were purchased from Sigma-Aldrich). PEG is a water soluble molecule that works as non ionic surfactant. Tween 20® is a polyoxyethylene derivate of sorbitan monolaurate, acts as surfactant and is widely used in biology to prevent non specific adsorption. Pluronic F-127® is a block copolymer based on polypropylene oxide and polyethylene oxide that works as non ionic surfactant. They three are biocompatible and are being used in biochemical applications.

The non-covalently functionalization of nanotubes was carried out by mixing the as-grown SWNTs with the corresponding surfactant in a 10 fold excess in milliQ water and stirred over 6 hours. Both stirring with a magnetic stirrer and in a sonication bath were used. The product was then filtered through a 3 μm pore size Isopore membrane filter and washed repeatedly with MilliQ water. The solid was then dried under vacuum.

3.2. Characterization

As-grown and functionalized SWNTs were characterized by several methods.

- Elemental Analisis provided information about the composition of the SWNTs. Carbon, hydrogen, nitrogen, sulphur and oxygen contents were measured with a Carlo Erba 1108 Elemental Analyzer.
- Inductively Coupled Plasma (ICP) provided information about the metal content. Nickel and Ytrium content was determined in a Jobin-Ybon 2000 ICP instrument.
- Fourier Transform Infrared Spectroscopy (FTIR) provided information about the functional groups present in the SWNTs, thus confirming the covalent functionalization of the material. FTIR was performed on a Bruker Vertex 70 instrument. All samples were prepared as pellets using spectroscopic grade KBr.
- Thermogravimetric Analysis (TGA) provided information about the percentage of surfactant surrounding the SWNTs or covalently bonded reagents, for both covalent and non covalent functionalization. TGA experiments were carried out with a SETARAM Setsys Evolution 16/18 device, heating from 0º to 1300ºC at 5ºC/min under nitrogen atmosphere.
- Transmission Electron Microscopy (TEM) images of some samples were taken. Micrographies were performed with a JEOL-2000 FXII electron microscope, working at 2000kV and with 0.28nm point-to-point resolution.
- Kaiser Test[67,68,58] was used to determine the number of free amine groups present in aminated SWNTs. A protocol adapted to our SWNTs was optimized.

3.3. Streptavidin adsorption test

The colorimetric method used to determine the non-specific adsorption is based on the horseradish peroxidase (HRP) catalyzed oxidation of 3,3',5,5'-tetramethylbenzidine (TMB)[69]. HRP is an enzyme specific for hydrogen acceptors. Only the H_2O_2, methyl- and ethyl- peroxides are actives. On the contrary, it is not specific for hydrogen donors, and reacts with a wide number of phenols, amino phenols, diamines, indophenols, leuko dyes, ascorbate and many amino acids. HRP catalyses the H_2O_2 oxidation of the TMB substrate by an electron transfer from the TMB to the peroxide giving a coloured product (Scheme 3). TMB has an absorbance maximum at 285 nm and the blue product obtained with one electron loss, gives absorbance peaks at 370nm and 652nm. The reaction can be stopped by H_2SO_4 addition, giving a yellow product with an absorbance maximum at 450nm.

Preliminary studies were performed in 2 mL eppendorf tubes. UV-vis measurements were carried out in a UV-vis Shimadzu UV-2401PC Spectrophotometer.

Semiquantitative studies were performed in 96-well filtering plates. UV-VIS measurements using the 96-well dishes were permorned in a SpectramaxPlus (Molecular Devices, Sunnyvale, CA).

The different types of nanotubes were dispersed in phosphate buffer solution 1x (PBS 1x). First, a study using different concentrations of SWNTs and streptavidin-peroxidase solution was carried out to determine the optimum ones. 50 μL of 100 μg/mL nanotubes dispersion and 50 μL of streptavidin-peroxidase solution of 0.04μg/mL were added to 96-well AcroWell^{TM} membrane-bottom plates with GHP (hydrophilic polyropilene) Membrane. These were the concentrations working better, and were the ones used in the experiments showed in this dissertation, were the final concentrations were 50 μg/mL for the SWNTs dispersions and 0.02 μg/mL for the streptavidin-peroxidase solution. After 30 minutes (900 rpm), the solution was filtered and washed four times with PBS buffer 1x to remove the streptavidin-peroxidase not adsorbed on the SWNTs. HRP buffer was fresh prepared and added over the SWNTs.

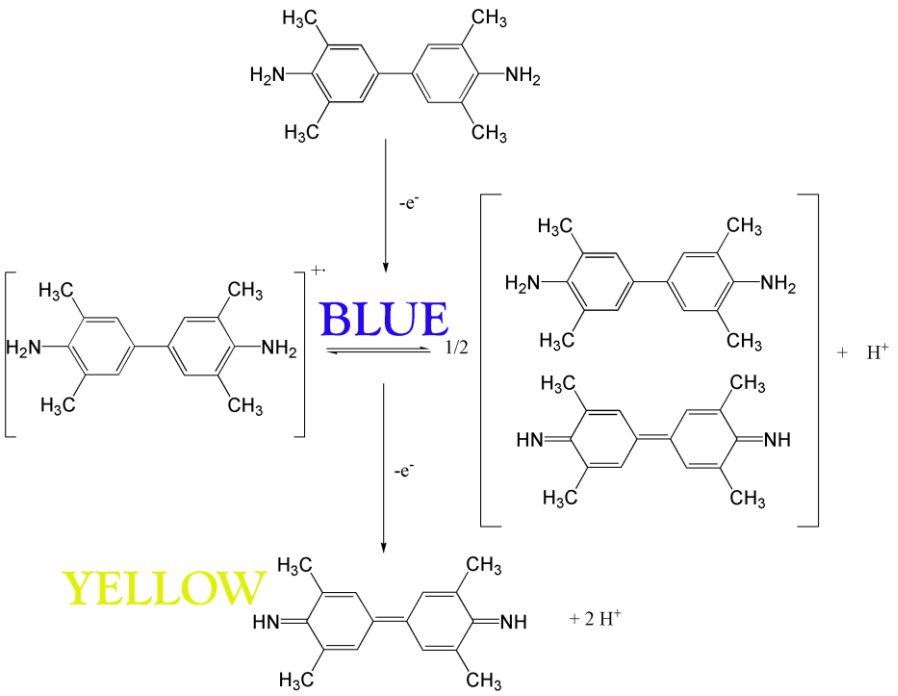

Scheme 3: TMB HRP catalyzed colorimetric test reaction.

HRP buffer consists on citrate buffer 1x, a 0.6% solution of TMB in dimethylsulfoxide (DMSO) and a 1% H_2O_2 solution. Blue colour was observed when streptavidin-peroxidase was present on the SWNTs. After 30 minutes the reaction was stopped by adding H_2SO_4 2M, and blue colour turned to yellow. After filtering, the absorbance was measured at 450.

Control experiments were also carried out to set the colour in the absence of nanotubes, due to the streptavidin-peroxidase adsorption on the filtering membrane material. This value has been substracted from the shown absorbance values.

The streptavidin adsorption onto the surface of the nanotubes was confirmed by addition of streptavidin doped with gold. As-grown SWNTs were mixed with streptavidin-gold (8-12 nm, Sigma-Aldrich) in PBS buffer 1x during 1 hour. After repeated centrifugation and redispersion to eliminate the excess of reactive, the nanotubes obtained were observed by TEM.

PBS buffer 1x consists on 10 mM phosphate buffer, pH 7.5. It was prepared by solving NaCl (8 g/L), KH_2PO_4 (0.2 g/L), Na_2HPO_4 (1.14 g/L) and KCl (0.2 g/L) in Milli-Q water.

Citrate buffer 1x consists on 0.04 M solution of sodium citrate in Milli-Q water, pH 5.5.

3.4. DNA adsorption and hybridization

Although the first idea had been to use the highly specific interaction between straptavidin and biotin to link biotin functionalized SWNTs to streptavidin of molecules functionalized with streptavidin, the results obtained had shown that this was not a good strategy. Streptavidin bonds non covalently SWNTs surface, and this interaction can't be completely hindered using surfactans.

As streptavidin attach to the SWNTs surface, and can't be removed by washing with detergent, we will use that interaction to bind biomolecules through the opposite strategy. SWNTs surface will be covered with streptavidin, and then biomolecules functionalized with biotin will be bound.

Using the highly specific interaction between streptavidin and biotin, streptavidin has been used as interlinker between SWNTs and a single stranded DNA (ssDNA) modified with biotin. The SWNTs used for this purpose have been acid treated to both oxidize and purify them. 1 mg of purified nanotubes were added to 1 mL of PBS 1x and sonicated during 4 hours. 200 μL of 1mg/mL streptavidin solution in PBS 1x was then added and let react during 1 hour under stirring in a sonication bath. The mixture was then spin-dried during 10 minutes at 13000 rpm. The supernatant was eliminated and the solid was washed twice with PBS 1x (sonication, centrifugation, removal of the supernatant).

The nanotubes covered with streptavidin were dispersed in 800 μL of PBS 2x and sonicated for 2 hours. Then 200 μL of a 75 μM solution of ssDNA-biotin solution in PBS 2x was added. The ssDNA-biotin used is a 20 bases molecule with the following sequence: CTC-GAT-GAC-TCA-ATG-ACT-CG with a biotin group in the 5' terminus. The mixture was allowed to react during 1 hour at room temperature under agitation. The mixture was then centrifuged for 10 minutes at 13000 rpm and washed twice with PBS 2x. The supernatant was eliminated.

Hybridization with the complementary strand was then performed. The complementary strand (CGA-GTC-ATT-GAG-TCA-TCG-AG) was functionalized in the 5' terminus with Alexa 555. This fluorescent dye has an absorption maximum at 555 nm and an emission maximum at 565 nm. 500 μL of a 15 μM solution of ss-DNA-Alexa 555 in SSC 2x was added. The mixture was agitated over night at 37ºC for DNA hybridization. The mixture was then centrifuged for 10 minutes at 13000 rpm and washed twice with SSC 0.1x to eliminate the non-hybridized strands.

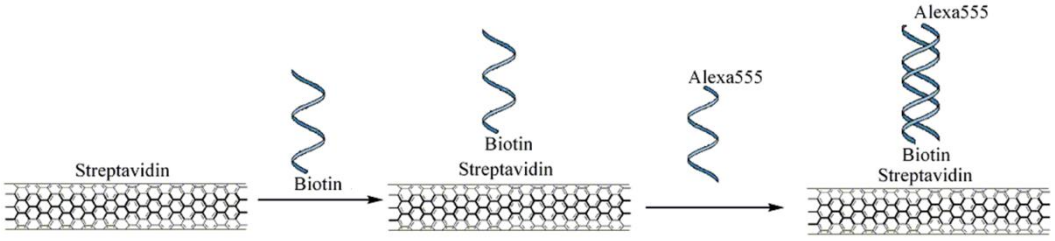

Scheme 4. DNA functionalization and hybridization.

Control experiment

In order to discard non specific adsorption of the fluorescent marked DNA strand on the surface of the nanotubes, a control experiment was carried out. The nanotubes covered with streptavidin were dispersed in 400μL of PBS 2x. Then 250 μL of the 15 μM ss-DNA-Alexa 555 solution were added and allowed to react for 1 hour at room temperature. The mixture was then centrifugated for 10 minutes at 13000 rpm and washed twice with PBS 2x.

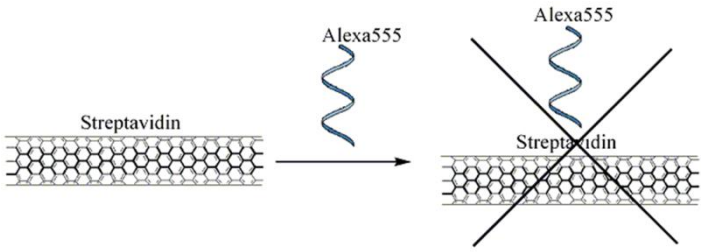

Scheme 5: Control experiment.

SSC buffer (saline-sodium citrate buffer) consists on NaCl and $Na_3C_6H_5O_7$ (trisodium citrate) at pH 7.0.

3.4.1 Micro contact printing

The solids obtained were dispersed in Milli-Q water, sonicated and diluted. Samples for observation at fluorescence microscope were prepared. Since SWNTs are too small to be observed in an optical microscope, conventional observation of the prepared solutions showed a uniform fluorescent/non fluorescent image not conclusive at all.

Micro contact printing[70] has been performed in order to completely discard that the obtained signal was noise. A PDMS (polydimethylsiloxane) stamp ($1cm^2$) with 5 μm spots design was used. The stamp was clean with EtOH and dried under N_2. The diluted solutions were then sonicated for 30 minutes and 100 μL were added over the stamps. Since the PDMS surface is highly hydrophobic, a glass cover slip was

carefully set on it to ensure complete contact of the solution with the stamp surface. After 1 hour contact, the stamp was washed with water and dried with N_2. Imprinting was then performed by putting the stamps upside down on a clean glass slide for 1 minute. (CORNING 2947-3x1. Micro Slides, Plain. Pre-Cleaned 3"x1". Thickness:0.96 to 1.06 mm. 0215 Glass, Approx. 1/2 Gross).

Observation at the fluorescence microscope was then performed. MIH Nikon Eclipse E1000 fluorescence microscope with MetaMorph software was used.

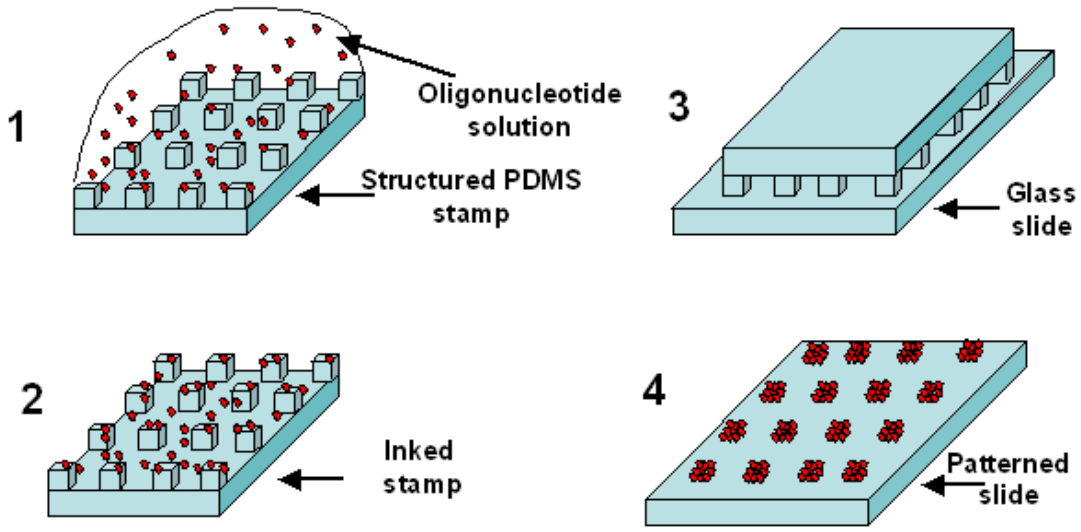

Figure 8: Micro contact printing of DNA molecules. 1) Inking of the stamp with the oligonucleotide solution, 2) drying of the stamp, 3) manual contact printing between the inked PDMS stamp and the glass slide, 4) DNA molecules are transferred on the slide along patterns that correspond to the relief structures in the PDMS stamp. (Reference 70)

4. Results and Discussion

4.1. Characterization of SWNTs

Elemental analysis of pristine and functionalized SWNTs and metal content of pristine and acid treated SWNTs is shown in Table 1.

	C	H	N	S	O	Ni	Y
As-produced SWNTs	84.1	0.2	0.2	0.0	1.5	9.1	3.6
Acid treated SWNTs	71.8	1.1	0.7	0.1	17.1	4.0	1.0
Aminated SWNTs	69.6	1.9	8.0	0.3	11.1	-	-
Biotinated SWNTs	69.5	3.3	10.3	2.9	11.6	-	-
Covalently functionalized PEG SWNTs	78.5	2.3	3.4	0.0	10.7	-	-
No covalently functionalized PEG SWNTs	78.4	1.2	0.3	0.0	-	-	-
No covalently functionalized PLURONIC ®F-127 SWNTs	75.5	2.6	0.2	0.0	-	-	-
No covalently functionalized TWEEN®20 SWNTs	77.3	2.5	0.3	0.0	-	-	-

Table 1: Elemental analysis of the employed materials.

After SWNTs oxidation with nitric acid, the oxygen content increases from 1.5 wt.% in pristine SWNTs to 17.1 wt.% in acid treated SWNTs. An increase in the nitrogen content is observed after reaction with ethylenediamine. After biotin functionalization, both an increase in the N and S content is observed. The number of free amine groups determined using the Kaiser test is 770 μmoles per gram of SWNTs. This value is an order of magnitude lower than the one calculated from elemental analysis. This could be due to SWNTs linking during functionalization, through diamine molecules bonding nanotubes at both ends.

The number of biotin groups calculated from the S content in the elemental analysis is of 888 μmoles of biotin groups per gram of SWNTs. This amount is consistent with the number of free amine groups determined by the Kaiser test. The SWNTs crosslinking during amine functionalization decreases the biotin SWNTs functionalization yield.

Figure 9 shows the FTIR spectra of the as produced SWNTs and covalently functionalized with oxygenated groups, amine groups, biotin groups and PEG. The band at ca. 1559 cm^{-1}, assigned to nanotubes C=C phonon modes[71], is observed in the as-produced SWNTs spectrum (Fig.9a). The presence of bands at ca. 3437 cm^{-1} and 1166 cm^{-1}, corresponding to O-H and C-O stretching modes, respectively, indicates the presence of some functional groups in the pristine SWNTs material. The appearance of bands ca. 3436 cm^{-1}, 1722 cm^{-1} and 1225 cm^{-1}, corresponding to O-H, C=O and C-O respectively, demonstrates the carboxylation of the SWNTs. (Fig.9b) After acylation and reaction with ethylenediamine, with formation of amide bonds, the band at ca. 1722 cm^{-1} due to C=O bond disappears and a shoulder at lower frequencies appears, ca. 1638 cm^{-1}, due to the amide carbonyl stretching mode. (Fig.9c) After reaction of the acylated SWNTs with the N-hydroxysuccinimidyl biotin, the two overlapped bands at ca. 1684 cm^{-1} and 1653 cm^{-1} are assigned to the carbonyl groups in amides located at different positions of the attached organic moieties (Fig.9d). The covalently PEG functionalized SWNTs shows the phonon modes from the nanotubes at ca. 1584 cm^{-1} and the bands due to C-O, C=O and O-H at ca. 1198 cm^{-1}, 1710 cm^{-1} and 3428 cm^{-1} respectively (Fig.9e).

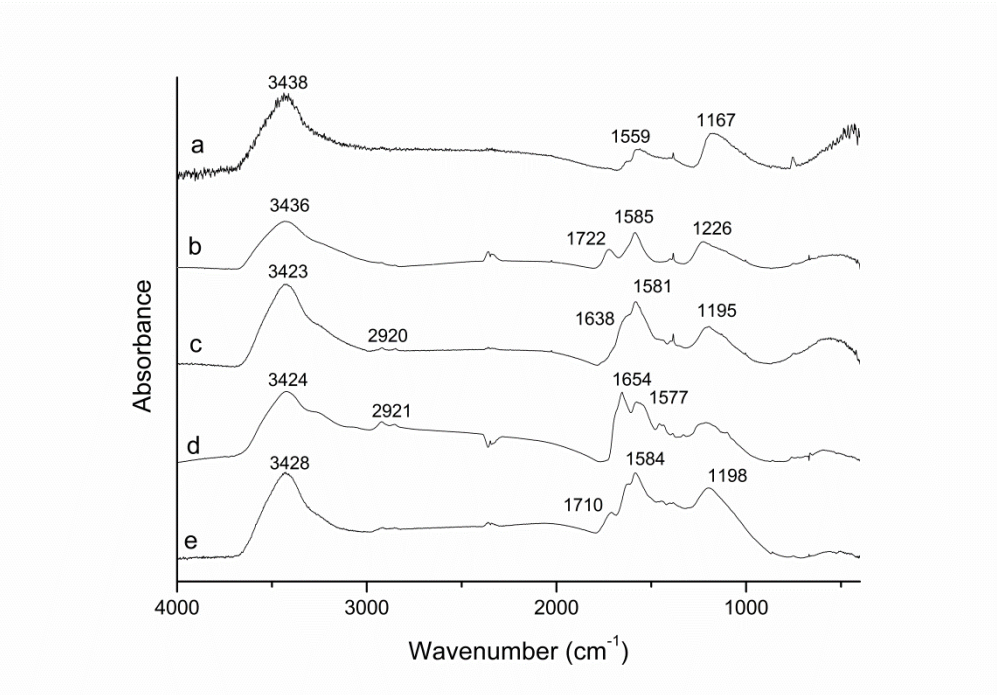

Figure 9: FTIR spectra of a) as-produced SWNTs, b) carboxylated SWNTs, c) aminated SWNTs, d) biotinated SWNTs and e) covalently functionalized SWNTs.

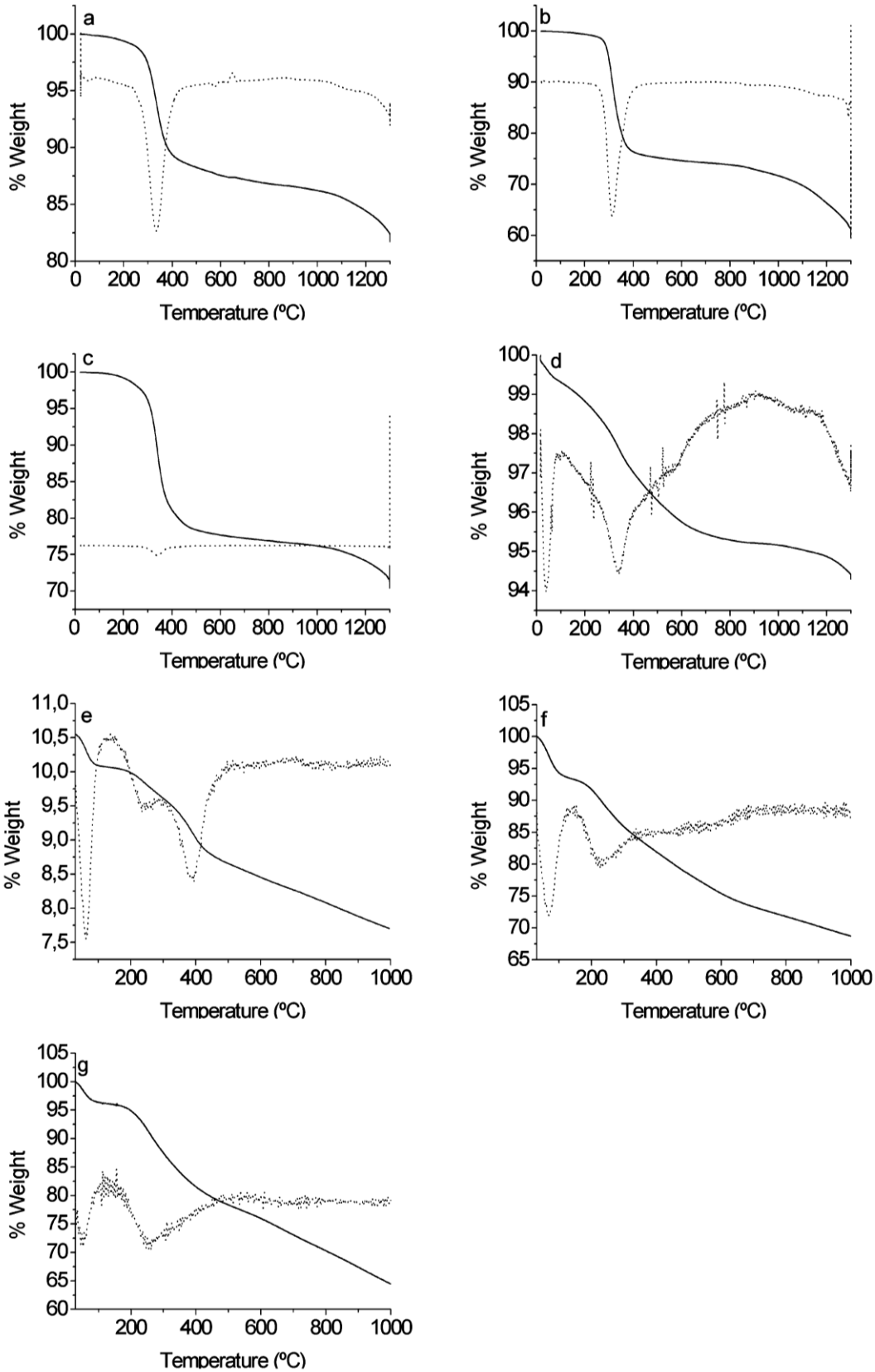

Figure 10: Nitrogen thermogravimetric analysis. TGA traces (solid line) and TGA derivates (doted line) of a) non-covalently PEG functionalized SWNTs, b) non covalently PLURONIC®F-127 functionalized SWNTs, c) non-covalently TWEEN®20 functionalized SWNTs, d) SWNTs as-grown, e) PEG covalently functionalized SWNTs, f) acid treated SWNTs, and g) aminated SWNTs.

The TGA analysis of the non-covalently functionalized nanotubes (Fig. 10a, b and c) shows a unique weight loss, and covalently functionalized nanotubes (Fig. 10e, f and g) show different behaviors.

TGA of pristine SWNTs (Fig. 10d) show a 0.6 wt. % loss at low temperature due to moisture loss, and a 5 wt. % loss at 341ºC due to the loss of functional groups existing in the as-grown material as indicated by the elemental analysis and FTIR. Non-covalently functionalized SWNTs with PEG, Pluronic® F-127 and Tween®20 show peaks at 335ºC, 314ºC and 340ºC respectively, and weight losses of 12%, 25% and 12% respectively, corresponding to the loss of non covalently adsorbed molecules on the CNTs as well as the functional groups existing in the as-grown SWNTs material. TGA of covalently PEG functionalized SWNTs (Fig. 10e) shows an initial 4.5 wt. % loss at low temperature due to moisture, and a 10 wt. % loss at 387ºC due to the PEG molecules covalently attached. The shoulder at ca. 250ºC is due to the loss of the remaining no functionalized carboxylic groups and oxydril groups and also possibly due to no covalently adsorbed PEG molecules. The TGA of acid treated SWNTs (Fig. 10f) shows a 13% weight loss at 226ºC corresponding to the removal of SWNTs oxygenated functional groups. The TGA of aminated SWNTs (Fig. 10g) show a 22% weight loss with the maximum at 255ºC corresponding to the loss of amine groups and remaining oxygenated groups.

TEM images obtained from the SWNTs treated with streptavidin-gold (Figure 11) shows the gold nanoparticles all along the nanotubes surface and the streptavidin wrapping the SWNTs bundles, thus confirming streptavidin adsorption on the carbon nanotubes surface.

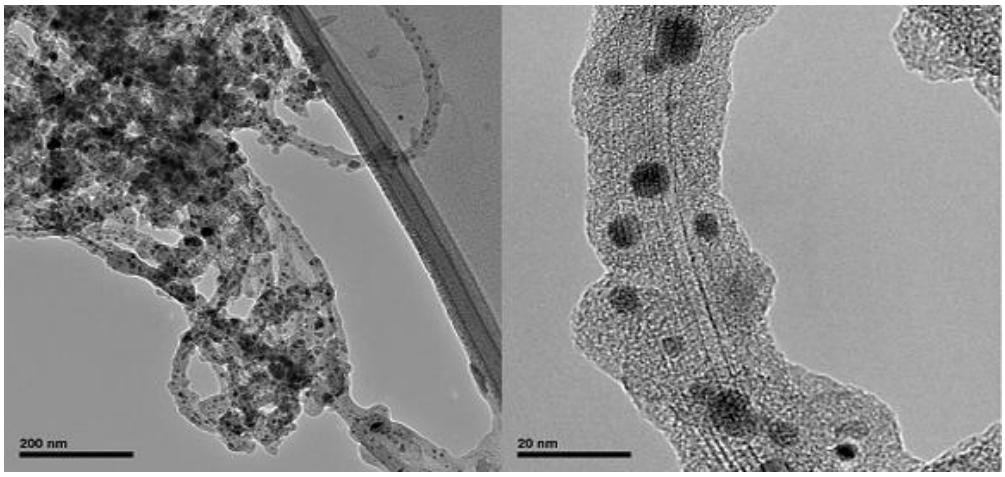

Figure 11: TEM image of streptavidin-gold coated SWNTs.

4.2. Streptavidin adsorption

The obtained results show that streptavidin adsorption took place in all the SWNTs materials studied. Blue color was observed, with different intensities depending on the functionalization of the SWNTs indicating that SWNTs surface modification considerably determines the streptavidin adsorption. Initially, qualitative studies were carried out, using 2 mL eppendorf tubes, in order to optimize the test procedure.

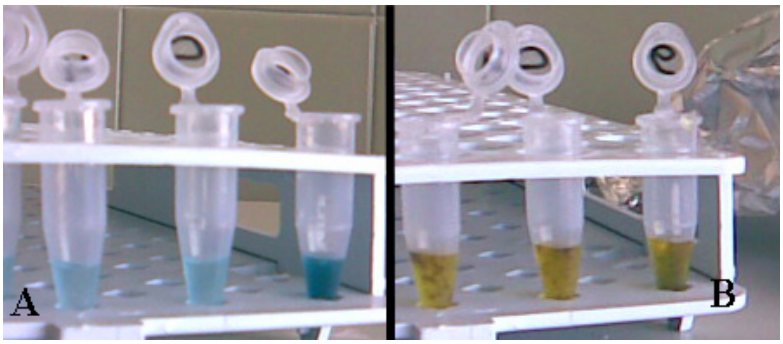

Figure 12: Color test for detecting the presence of streptavidin. A)Before and B) after adition of H_2SO_4.

Semiquantitative analyses were performed in 96-well filtering plates. The first step was to optimize the SWNTs and streptavidin-HRP concentration for the volume of the wells.

A first 2D (two dimensional, the influence of the concentration of both solutions used in the reactions was studied) experiment was carried out using 100 μg/mL, 20 μg/mL and 4 μg/mL of SWNT-COOH and SWNT-biotin, and 10 μg/mL , 2 μg/mL and 0.4 μg/mL of streptavidin-HRP. Distribution of wells is shown in Table 2. Results are shown in Figure 13. No significant difference between the two types of nanotubes was observed. Signal saturation was observed at low streptavidin-HRP concentration. Dilution of this reactive in a factor of 10 was performed.

A second 2D experiment was carried out using 100 μg/mL, 20 μg/mL and 4 μg/mL of SWNT-COOH and SWNT-biotin, and 1 μg/mL, 0.2 μg/mL and 0.04 μg/mL of streptavidin-HRP. Distribution of wells is shown in Table 3. Results are shown in Figure 14. Acceptable absorbance values and enough difference for the two types of nanotubes is observed for 100 μg/mL of nanotubes and 0.04 μg/mL of streptavidin-HRP.

	4	5	6	7
A	50 µL SWNT-biotina 100 µg/mL + 50 µL strept-HRP 10 µg/mL	50 µL SWNT-biotina 100 µg/mL + 50 µL strept-HRP 2 µg/mL	50 µL SWNT-biotina 100 µg/mL + 50 µL strept-HRP 0.4 µg/mL	50 µL SWNT-biotina 100 µg/mL + 50 µL PBS 1x
B	50 µL SWNT-biotina 20 µg/mL + 50 µL strept-HRP 10 µg/mL	50 µL SWNT-biotina 20 µg/mL + 50 µL strept-HRP 2 µg/mL	50 µL SWNT-biotina 20 µg/mL + 50 µL strept-HRP 0.4 µg/mL	50 µL SWNT-biotina 20 µg/mL + 50 µL PBS 1x
C	50 µL SWNT-biotina 4 µg/mL + 50 µL strept-HRP 10 µg/mL	50 µL SWNT-biotina 4 µg/mL + 50 µL strept-HRP 2 µg/mL	50 µL SWNT-biotina 4 µg/mL + 50 µL strept-HRP 0.4 µg/mL	50 µL SWNT-biotina 4 µg/mL + 50 µL PBS 1x
D	50 µL PBS 1x + 50 µL strept-HRP 10 µg/mL	50 µL PBS 1x + 50 µL strept-HRP 2 µg/mL	50 µL PBS 1x + 50 µL strept-HRP 0.4 µg/mL	50 µL PBS 1x + 50 µL PBS 1x
E	50 µL SWNT-COOH 100 µg/mL + 50 µL strept-HRP 10 µg/mL	50 µL SWNT-COOH 100 µg/mL + 50 µL strept-HRP 2 µg/mL	50 µL SWNT-COOH 100 µg/mL + 50 µL strept-HRP 0.4 µg/mL	50 µL SWNT-COOH 100 µg/mL + 50 µL PBS 1x
F	50 µL SWNT-COOH 20 µg/mL + 50 µL strept-HRP 10 µg/mL	50 µL SWNT-COOH 20 µg/mL + 50 µL strept-HRP 2 µg/mL	50 µL SWNT-COOH 20 µg/mL + 50 µL strept-HRP 0.4 µg/mL	50 µL SWNT-COOH 20 µg/mL + 50 µL PBS 1x
G	50 µL SWNT-COOH 4 µg/mL + 50 µL strept-HRP 10 µg/mL	50 µL SWNT-COOH 4 µg/mL + 50 µL strept-HRP 2 µg/mL	50 µL SWNT-COOH 4 µg/mL + 50 µL strept-HRP 0.4 µg/mL	50 µL SWNT-COOH 4 µg/mL + 50 µL PBS 1x
H	50 µL PBS 1x + 50 µL strept-HRP 10 µg/mL	50 µL PBS 1x + 50 µL strept-HRP 2 µg/mL	50 µL PBS 1x + 50 µL strept-HRP 0.4 µg/mL	50 µL PBS 1x + 50 µL PBS 1x

Table 2: First 2D experiment for adjusting the reactives concentration.

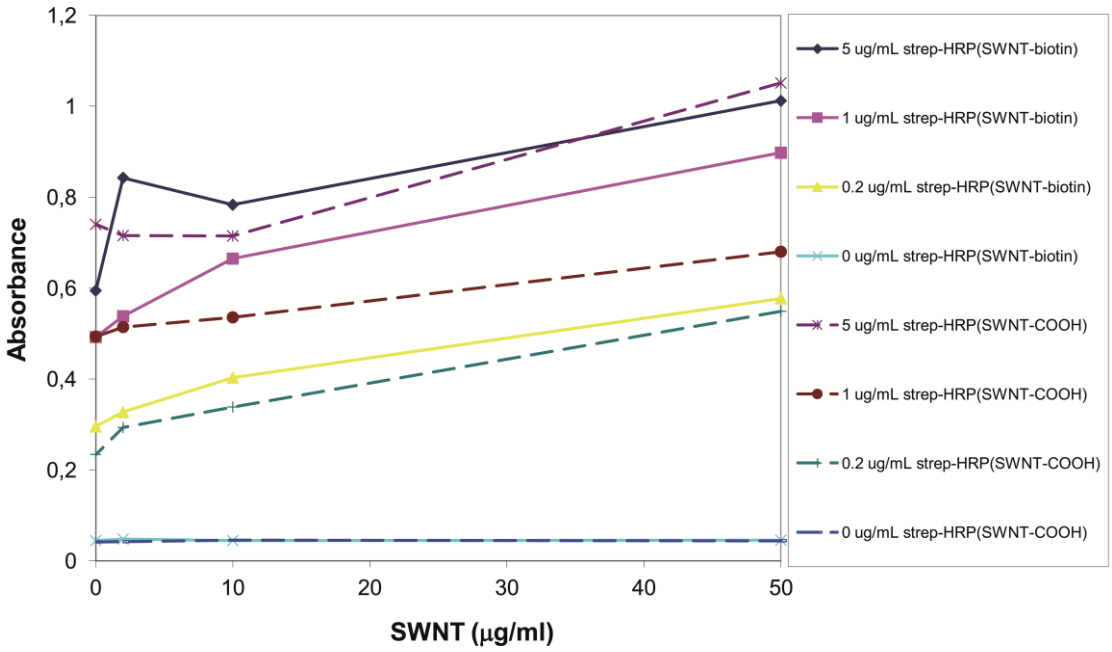

Figure 13: Results from the first 2D experiment.

	4	5	6	7
A	50 µL SWNT-biotina 100 µg/mL + 50 µL strept-HRP 1 µg/mL	50 µL SWNT-biotina 100 µg/mL + 50 µL strept-HRP 0.2 µg/mL	50 µL SWNT-biotina 100 µg/mL + 50 µL strept-HRP 0.04 µg/mL	50 µL SWNT-biotina 100 µg/mL + 50 µL PBS 1x
B	50 µL SWNT-biotina 20 µg/mL + 50 µL strept-HRP 1 µg/mL	50 µL SWNT-biotina 20 µg/mL + 50 µL strept-HRP 0.2 µg/mL	50 µL SWNT-biotina 20 µg/mL + 50 µL strept-HRP 0.04 µg/mL	50 µL SWNT-biotina 20 µg/mL + 50 µL PBS 1x
C	50 µL SWNT-biotina 4 µg/mL + 50 µL strept-HRP 1 µg/mL	50 µL SWNT-biotina 4 µg/mL + 50 µL strept-HRP 0.2 µg/mL	50 µL SWNT-biotina 4 µg/mL + 50 µL strept-HRP 0.04 µg/mL	50 µL SWNT-biotina 4 µg/mL + 50 µL PBS 1x
D	50 µL PBS 1x + 50 µL strept-HRP 1 µg/mL	50 µL PBS 1x + 50 µL strept-HRP 0.2 µg/mL	50 µL PBS 1x + 50 µL strept-HRP 0.04 µg/mL	50 µL PBS 1x + 50 µL PBS 1x
E	50 µL SWNT-COOH 100 µg/mL + 50 µL strept-HRP 1 µg/mL	50 µL SWNT-COOH 100 µg/mL + 50 µL strept-HRP 0.2 µg/mL	50 µL SWNT-COOH 100 µg/mL + 50 µL strept-HRP 0.04 µg/mL	50 µL SWNT-COOH 100 µg/mL + 50 µL PBS 1x
F	50 µL SWNT-COOH 20 µg/mL + 50 µL strept-HRP 1 µg/mL	50 µL SWNT-COOH 20 µg/mL + 50 µL strept-HRP 0.2 µg/mL	50 µL SWNT-COOH 20 µg/mL + 50 µL strept-HRP 0.04 µg/mL	50 µL SWNT-COOH 20 µg/mL + 50 µL PBS 1x
G	50 µL SWNT-COOH 4 µg/mL + 50 µL strept-HRP 1 µg/mL	50 µL SWNT-COOH 4 µg/mL + 50 µL strept-HRP 0.2 µg/mL	50 µL SWNT-COOH 4 µg/mL + 50 µL strept-HRP 0.04 µg/mL	50 µL SWNT-COOH 4 µg/mL + 50 µL PBS 1x
H	50 µL PBS 1x + 50 µL strept-HRP 1 µg/mL	50 µL PBS 1x + 50 µL strept-HRP 0.2 µg/mL	50 µL PBS 1x + 50 µL strept-HRP 0.04 µg/mL	50 µL PBS 1x + 50 µL PBS 1x

Table 3: Second 2D experiment for adjusting the reactives concentracion.

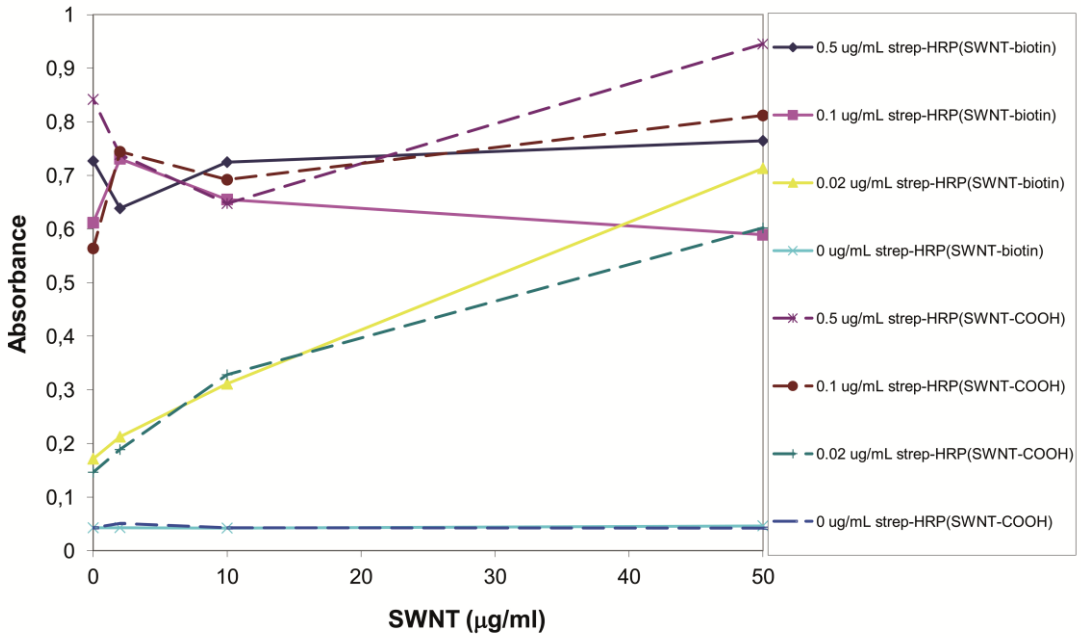

Figure 14: Results from the second 2D experiment.

Final experiments were performed by triplicate in order to ensure the reproducibility of the results. 100 μg/mL of carbon nanotubes and 0.04 μg/mL of streptavidin-HRP. This means final concentrations of 50 μg/mL of nanotubes and 0.02 μg/mL of streptavidin-HRP.

Figure 15 shows the adsorption of streptavidin-peroxidase on the different SWNTs used.

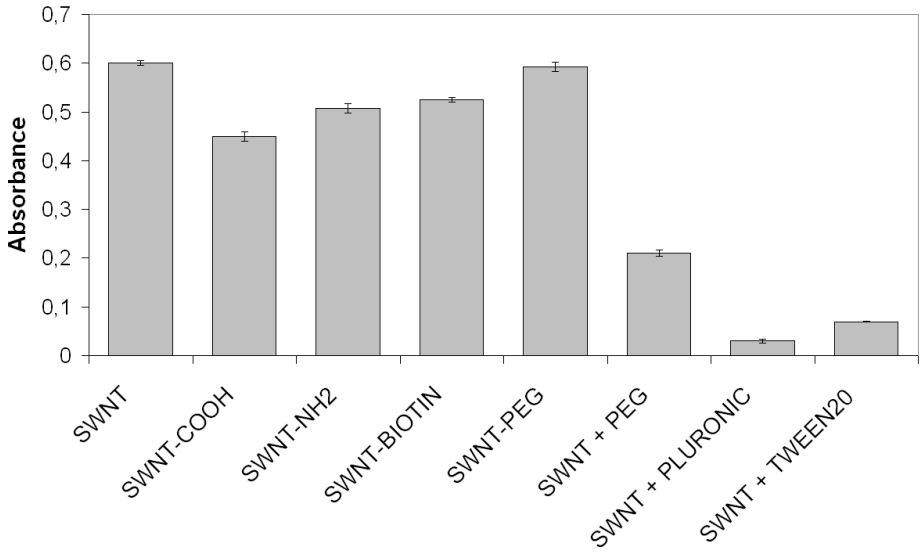

Figure 15: Streptavidin-peroxidase adsorption on different SWNTs samples.

A small adsorption was observed in the control experiments when only PBS 1x was added to the well due to filter membrane material adsorption. This adsorption is substracted from the values showed in Figure 15. As expected, adsorption was most effectively prevented by non-covalent functionalization, even though it was not completely hindered. The different groups present on the surface in the covalently functionalized SWNTs showed differences in adsorption. These differences can be attributed to different hydrophobic character, resulting in higher adsorption on as grown SWNTs surface due to their high hydrophobicity. Unexpectedly, adsorption on biotinated SWNTs was not significantly higher confirming the important non-specific absorption of the streptavidin on SWNTs walls.

Streptavidin is a 60 KDa tetrameric protein obtained from *Streptomyces avidinii*. Streptavidin is 5 nm diameter and many amino and carboxylic groups, which are able to bind SWNTs surface. The type of interaction may vary depending on the surface functionalization. For the as-produced SWNTs, hydrophobic interactions are

probably responsible for non-specific adsorption, whereas for carboxylic and amino functionalized SWNTs, acid-base interactions may also participate in the adsorption. Azamian et al.[72] have reported that the adsorption of proteins on SWNTs happens with both positively and negatively charged proteins with such strong adsorption being consistent with an electrostatic adsorption mechanism. The observed proteins adsorption seems to be at least in part associated with the amino affinity of carbon nanotube.

A comprehensive understanding of the non-specific protein-carbon nanotube interactions requires more investigations at the molecular level. For example, different amino acid residue compositions and sequences may vary the adsorption on surfaces. In addition, the secondary (and maybe tertiary and quaternary) structures of the proteins may affect the non-specific interactions and related properties. The same molecular level investigation is also required for an improved understanding of the role of the nanotube electronic structures in the interactions.

4.3. DNA hybridization

DNA adsorption and hybridization processes were carried out. Micro contact printing was performed with the solutions obtained from hybridization and control experiments.

For the control experiment no fluorescence was observed, thus discarding direct adsorption of de labeled single DNA strand on the surface of the streptavidin covered SWNTs. As ssDNA adsorbs on the surface of bare SWNTs, thus mean effective covering of the surface by the streptavidin.

Fluorescence was observed for the hybridization experiment (Figure 16), thus confirming hybridization of the DNA linked to the SWNTs by the biotin-streptavidin system.

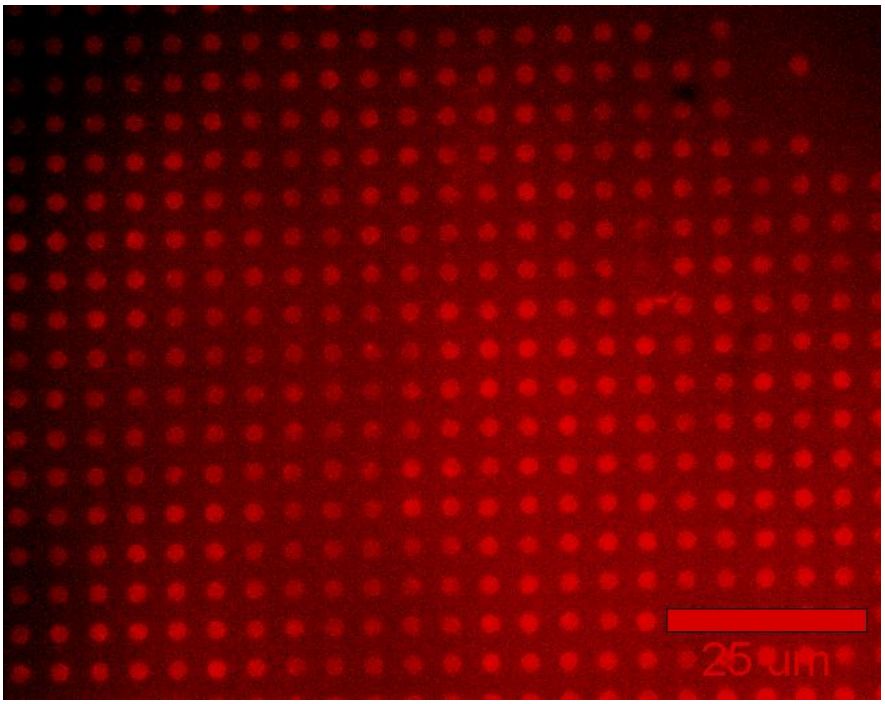

Figure 16: Fluorescent image of the imprinted hybridized DNA SWNTs.

5. Conclusions

SWNTs have been covalently functionalized with carboxylic groups, amine groups and PEG, and no covalently functionalized with PEG, Pluronic® F-127 and Tween®20. FTIR spectra have confirmed the SWNTs covalent functionalization and TGA have confirmed the non covalent functionalization. Elemental analysis together with the Kaiser test indicated that some crosslinking between SWNTs occurs during the amination step, leading to a lower number of free amine groups available for binding the biotin. The blockage of amine groups would lead to higher biotin SWNTs functionalization yields.

Streptavidin adsorbs non specifically on the surface of the as-grown SWNTs as well as on the acid treated, aminated, and PEG covalently functionalized SWNTs. Adsorption is higher on as grown SWNTs due to their higher hydrophobicity. PEG, Pluronic® F-127 and Tween®20 non covalently functionalized SWNT shows low adsorption of streptavidin, nevertheless no complete blockage of this adsorption has been achieved. The streptavidin adsorption on biotinated SWNTs is of the same order than on raw SWNTs indicating the strong non-specific adsorption of streptavidin on SWNTs walls.

The highly specific biotin-streptavidin interaction, led us to the utilization of streptavidin as interlinker between SWNTs and bioreceptor molecules. This has been used to link a single strand of DNA to the SWNT.

Hybridization of the DNA has been performed and non specific adsorption of DNA has been ruled out.

This strategy has been also used to anchor DNA strand to SWNTs in FETs for building DNA electronic biosensors[73].

6. References

1. H.W. Kroto, J.R. Heath, S.C. Obrien, R.F. Curl, R.E. Smalley, C_{60}Buckminsterfullerene, *Nature*, **1985**, 318, 162-163.
2. S. Iijima, Helical Microtubules of Graphitic Carbon, *Nature,* **1991**, 354, 56-58.
3. D.S. Bethune, C.H. Kiang, M.S. Devries, G. Gorman, R. Savoy, J. Vazquez, R. Beyers, Cobalt-Catalyzed Growth of Carbon Nanotubes with Single-Atomic Layerwalls, *Nature*, **1993**, 363, 605-607.
4. S. Iijima, T. Ichihashi, Single-Shell Carbon Nanotubes of 1nm Diameter, *Nature,* **1993**, 363, 603-605.
5. S. Iijima, Growth of Carbon Nanotubes, *Materials Science and Engineering B*, **1993**, 19, 172-180.
6. R. Saito, G. Dresselhaus, M.S. Dresselhaus, Physics of carbon nanotubes, *Carbon*, **1995**, 33, 883-891.
7. R. Saito, G. Dresselhaus, M.S. Dresselhaus, Tunneling conductance of connected carbon nanotubes, *Physical Review B*, **1996**, 53, 2044-2050.
8. W. Kim, H.C. Choi, M. Shim, Y. Li, D. Wang, H. Dai, Synthesis of ultralong and high percentage of semiconducting single-walled carbon nanotubes, *Nano Letters,* **2002**, 2 (7), 703-708.
9. A. Krishnan, E. Dujardin, T.W. Ebbesen, P.N. Yianilos, M.M.J. Treacy, Young's modulus of single-walled nanotubes, *Physical Review B*, **1998**, 58, 14013-14019.
10. B.I. Yakobson, C.J. Brabec, J. Bernholc, Nanomechanics of carbon tubes: Instabilities beyond linear response, *Physical Review Letters*, **1996**, 76, 2511-2514.
11. M.B. Nardelli, J.L. Fattebert, D. Orlikowski, C. Roland, Q. Zhao, J. Bernholc, Mechanical properties, defects and electronic behavior of carbon nanotubes, *Carbon*, **2000**, 38, 1703-17011.
12. R.S. Ruoff, D.C. Lorents, Mechanical and thermal properties of carbon nanotubes, *Carbon*, **1995**, 33, 925-930.
13. S. Frank, P. Poncharal, Z.L. Wang, W.A. de Heer, Carbon nanotube quantum resistors, *Science*, **1998**, 280, 1744-1746.

14. H.S. Philip Wong, D. Akinwande, "Carbon Nanotube and Graphene Device Physics", Chapter 9: Applications of carbon nanotubes, Cambridge University Press, **2011**.

15. F. Liang, B. Chen, A review on biomedical applications of singlewalled carbon nanotubes, *Current Medicinal Chemistry*, **2010**, 17, 10-24.

16. S. Niyogi, M.A. Hamon, H. Hu, B. Zhao, P. Bhowmik, R. Sen, M.E. Itkis, R.C. Haddon, Chemistry of single-walled carbon nanotubes, *Accounts of Chemical Research*, **2002**, 35, 1105-1113.

17. D. Tasis, N. Tagmatarchis, A. Bianco, M. Prato, Chemistry of carbon nanotubes, *Chemical Reviews*, **2006**, 106, 1105-1136.

18. P.J. Boul, J. Liu, E.T. Mickelson, L.M. Ericson, I.W. Chiang, K.A. Smith, D.T. Colbert, R.H. Hauge, J.L. Margrave, R.E. Smalley, Reversible sidewall functionalization of buckytubes, *Chemical Physics Letters*, **1999**, 310, 367-372.

19. J.L. Bahr, J. Yang, D.V. Kosynkin, M.J. Bronikowski, R.E. Smalley, J.M. Tour, Functionalization of carbon nanotubes by electrochemical reduction of aryl diazonium salts: A bucky paper electrode, *Journal of the American Chemical Society*, **2001**, 123, 6536-6542.

20. M. Holzinger, O. Vostrowsky, A. Hirsch, F. Hennrich, M. Kappes, R. Weiss, F. Jellen, Sidewall functionalization of carbon nanotubes, *Angewandte Chemie International Edition* **2001**, 40, 4002.

21. P. Calvert, Nanotube composites-A recipe for strength, *Nature* **1999**, 399, 210-211.

22. N. Nakashima, Y. Tomonari, H. Murakami, Water-soluble single-walled carbon nanotubes via noncovalent sidewall-functionalizationwith a pyrene-carrying ammonium ion, *Chemistry Letters*, **2002**, 638-639.

23. A.B. Dalton, C. Stephan, J.N. Coleman, B. McCarthy, P.M. Ajayan, S. Lefrant, P. Bernier, W.J. Blau, H.J. Byrne, Selective interaction of a semiconjugated organic polymer with single-walled nanotubes, *Journal of Physical Chemistry B*, **2000**, 104, 10012-100016.

24. J.M. Bonard, T. Stora, J.B. Salvetat, F. Maier, T. Stockli, C. Duschl, L. Forro, W.A. de Heer, A. Chatelain, Purification and size-selection of carbon nanotubes, *Advanced Materials*, **1997**, 9, 827

25. G.R. Dieckmann, A.B. Dalton, P.A. Johnson, J. Razal, J. Chen, G.M. Giordano, E. Muñoz, I.H. Musselman, R.H. Baughman, R.K. Draper, Controlled assembly of carbon nanotubes by designed amphiphilic peptide helices, *Journal of the American Chemical Society*, **2003**, 125, 1770-1777.

26. M. Zheng, A. Jagota, E.D. Semke, B.A. Diner, R.S. McLean, S.R. Lustig, R.E. Richardson, N.G. Tassi, DNA-assisted dispersion and separation of carbon nanotubes, *Nature Materials*, **2003**, 2, 338-342.

27. D. Cattopadhyay, I. Galeska, F. Papadimitrakopoulos, A route for bulk separation of semiconducting from metallic single-walled carbon nanotubes, *Journal of the American Chemical Society*, **2003**, 125, 3370-3375.

28. H. Dumortier, S. Lacotte, G. Pastorin, R. Marega, W. Wu, D. Bonifazi, J.P. Briand, M. Prato, S. Muller, A. Bianco, Functionalized carbon nanotubes are non-cytotoxic and preserve the functionality of primary immune cells, *Nano Letters*, **2006**, 6(7), 1522-1528.

29. C.M. Sayes, F. Liang, J.L. Hudson, J. Mendez, W.H. Guo, J.M. Beach, V.C. Moore, C.D. Doyle, J.L. West, W.E. Billups, K.D. Ausman, V.L. Colvin, Functionalization density dependence of single-walled carbon nanotubes cytotoxicity in vitro, *Toxicology Letters*, **2006**, 131, 2, 135-142.

30. Y. Yan, W. Zheng, M. Zhang, L. Wang, L. Su, L. Mao, Bioelectrochemically functional nanohybrids through co-assembling of proteins and surfactants onto carbon nanotubes: facilitated electron transfer and assembled proteins with enhanced faradic response, *Langmuir* **2005**, 21, 6560-6566.

31. N.W.S. Kam, H. Dai, Carbon nanotubes as intracellular protein transporters: generality and biological functionality, *Journal of the American Chemical Society*, **2005**, 127, 6021-6026.

32. K. Besteman, J.-O. Lee, F.G.M. Wiertz, H.A. Heering, C. Dekker, Enzyme-coated carbon nanotubes as single-molecule biosensors, *Nano Letters*, **2003**, 3, 727-730.

33. F. Balavoine, P. Schultz, C. Richard, V. Mallouh, T.W. Ebbesen, C. Mioskowski, *Angew. Chem. Int. Ed.* **1999**, 38, 1912

34. S.S. Karajanagi, A.A. Vertegel, R.S. Kane, J.S. Dordick, Structure and function of enzymes adsorbed onto single-walled carbon nanotubes, *Langmuir, **2004**,* 20, 11594-11599.

35. Y. Lin, L.F. Allard, Y.-P. Sun, Protein-affinity of single-walled carbon nanotubes in water, *The Journal of Physical Chemistry B*, **2004**, 108, 3760-3764.
36. K. Fu, W. Huang, Y. Lin, D. Zhang, T.W. Hanks, A.M. Rao, Y.P. Sun, Functionalization of carbon nanotubes with bovine serum albumin in homogeneous aqueous solution, *Journal of Nanoscience and Nanotechnology*, **2002**, 2, 457-461.
37. M. Shim, N. Wong Shi Kam, R.J. Chen, Y. Li, H. Dai, Functionalization of carbon nanotubes for biocompatibility and biomolecular recognition, *Nano Letters*, **2002**, Vol.2, No.4, 285-288.
38. J.J. Davis, J.L.H. Green, H.A.O. Hill, Y.C. Leung, P.J. Sadler, J. Sloan, A.V. Xavier, S.C. Tsang,The immobilisation of proteins in carbon nanotubes, *Inorganica Chimica Acta*, **1997**, 272, 261-266.
39. Y.Lin, S. Talylor, H. Li, K.A. S. Fernanddo, L. Qu, W. Wang, L. Gu, B. Zhou Y.P. Sun, Advances towards bioapplications of carbon nanotubes, *Journal of Materials Chemistry*, **2004**, 14, 527-541.
40. N.L. Anderson, N.G. Anderson, The human plasma proteome, *Mollecular & Cellular Proteomics*, **2002**, 1, 845-867.
41. J.N.Adkins, S.M. Varnum, K.J. Auberry, R.J. Moore, N.H. Angell, R.D. Smith, D.L. Springer, J.G. Pounds, Toward a human blood serum proteome, *Molecular & Cellular Proteomics*, **2002**, 1, 947-955.
42. A. Bogomolova, E. Komarova, K. Reber, T. Gerasimov, O. Yavuz, S. Bhatt, M. Aldissi, Challenges of electrochemical impedance spectroscopy in protein biosensing**,** *Analytical Chemistry***, 2009**, 81, 3944-3949.
43. M. Mrksich, G.M. Whitesides, Using self-assembled monolayers that present oligo(ethylene glycol) groups to control the interactions of proteins with surfaces, *Poly(ethylene glycol), ACS Symposium Series* **1997**, Vol.680, 361-373.
44. E. Ostuni, R.G. Chapman, R.E. Holmlin, S. Takayama, F.M. Whitesides, A survey of structure-property relationships of surfaces that resist the adsorption of protein, *Langmuir*, **2001**, 17, 5605-5620.
45. R.J. Chen, S. Bangsaruntip, K.A. Drouvalakis, N.W.S. Kim, M. Shim, Y. Li, W. Kim, P.J. Utz, H. Dai, Noncovalent functionalization of carbon nanotubes for highly specific electronic biosensors, *Proceedings of the National Academy of Sciences USA*, **2003**, 100, 4984-4989.

46. David A. Britz and Andrei N. Khlobystov, Noncovalent interactions of molecules with single walled carbon nanotubes, *Chemical Society Reviews*, **2006**, 35, 637-659.

47. W. Wenseleers, I.I. Vlasov, E. Goovaerts, E.D. Obraztsova, A.S. Lobach, A. Bouwen, Efficient isolation and solubilisation of pristine single-walled nanotubes in bile salt micelles, *Advanced Functional Materials*, **2004**, 14, 1105-1112.

48. M.F. Islam, E. Rojas, D.M. Bergey, A.T. Johnson, A.G. Yodh, High weight fraction surfactant solubilisation of single-wall carbon nanotubes in water, *Nano Letters*, **2003**, 3, 269-273.

49. A.Erdem, P. Papakonstantinou, H. Murphy, M. McMullan, H. Karadeniz, S. Sharma, Streptavidin modified carbon nanotube based graphite electrode for label-free sequence specific DNA detection, *Electroanalysis*, **2010,** 22, 6, 611-617.

50. Z. Liu, F. Galli, K.G.H. Janssen, L Jiang, H. J. van der Linden, D.C. de Geus, P. Voskamp, M.E. Kuil, R.C.L. Olsthoorn, T.H. Oosterkamp, T. Hankemeier, J.P. Abrahams, Stable single-walled carbon nanotube-streptavidin complex for biorecognition, *Journal of Physical Chemistry C*, **2010**, 114, 4345-4352.

51. W. Gao, H. Dong, J. lei, H. Ji, H. Ju, Signal amplification of streptavidin-horseradish peroxidase functionalized carbon nanotubes for amperometric detection of attomolar DNA, *Chemical Communications*, **2011**, 47, 5220-5222.

52. H.S. Philip Wong, D. Akinwande, "Carbon Nanotube and Graphene Device Physics", Chapter 8: Carbon nanotube field-effect transistors, Cambridge University Press, **2011**.

53. http://www.britannica.com/EBchecked/media/147/Perspective-of-a-MOSFET-with-symbols-for-n-and-p

54. S.J. Tans, A.R.M. Verschueren, C. Dekker, Room-temperature transistor based on a single carbon nanotube, *Nature*,**1998**, 393, 49-52.

55. R. Martel, T. Schmidt, H.R. Shea, T. Hertel, P. Avouris, Single- and multi-wall carbon nanotube field-effect transistors, *Applied Physics Letters*, **1998**, 73, 2447-2449.

56. G. Gruner, Carbon nanotube transistors for biosensing applications, *Analytical and Bioanalytical Chemistry*, **2006**, 384, 322-335.

57. D.R. Kauffman, A. Star, Electronically monitoring biological interactions with carbon nanotube field-effect transistors, *Chemical Society Reviews*, **2008**, 37, 1197-1206.

58. D. Pantarotto, C.D. Partidos, R. Graff, J. Hoebeke, J.-P. Briand, M. Prato, A. Bianco, Synthesis, structural characterization, and immunological properties of carbon nanotubes functionalized with peptides, *Journal of the American Chemical Society*, **2003**, 125, 6160-6164.

59. F.N. Ishikawa, M. Curreli, C.A. Olson, H-I. Liao, R. Sun, R.W. Roberts, R.J. Cote, M.E. Thompson, C. Zhou, Importance of controlling nanotube density for highly sensitive and reliable biosensors functional in physiological conditions, *ACS Nano,* **2010**, 4, 11, 6914-6922.

60. M.T. Martínez, Y-C. Tseng, J.P. Salvador, M.P. Marco, N. Ormategui, I. Loinaz, J. Bokor, Electronic anabolic steroid recognition with carbon nanotube field-effect transistors, *ACS Nano*, **2010**, 4, 3, 1473-1480.

61. M.T. Martínez, Y-C. Tseng, N. Ormategui, I. Loinaz, R. Eritja, J. Bokor, Label-free DNA biosensors based on functionalized carbon nanotube field effect transistors, *Nano Letters*, **2009**, 9, 2, 530-536.

62. C. Journet, W.K. Maser, P. Bernier, A. Loiseau, M. Lamy de la Chapelle, S. Lefrant, Large-scale production of single-walled carbon nanotubes by the electric-arc technique, *Nature*, **1997**, 388, 756-758.

63. A.M. Benito, W.K. Maser, M.T. Martínez, Carbon nanotubes: from production to functional composites, *International Journal of Nanotechnology***, 2005,** 2, 71-89.

64. M.T. Martínez, M.A. Callejas, A.M. Benito, M. Cochet, T. Seeger, A. Ansón, J. Schreiber, C. Gordon, C. Marhic, O. Chauvet, W.K. Maser, Modifications of single-wall carbon nanotubes upon oxidative purification treatments, *Nanotechnology* **2003**, 14, 691-695.

65. M.T. Martínez, M.A. Callejas, A.M. Benito, M. Cochet, T. Seeger, A. Ansón, J. Schreiber, C. Gordon, C. Marhic, O. Chauvet, J.L.G. Fierro, W.K. Maser, Sensitivity of single wall carbon nanotubes to oxidative processing: structural modification, intercalation and functionalisation, *Carbon* **2003**, 41, 2247-2256.

66. Montesa, E. Muñoz, A.M. Benito, W.K. Maser, M.T. Martínez, FTIR and thermogravimetric analysis of biotin-functionalized single-walled carbon

nanotubes, *Journal of Nanoscience and Nanotechnology*, **2007**, Vol. 7, Iss. 10, 3473-3476.

67. E. Kaiser, R.L. Colescott, C.D. Bossinger, P.I. Cook, Color test for detection of frère terminal amino groups in the solid-phase of peptides, *Analytical Biochemistry*, **1970**, 34, 595-598.
68. V.K. Sarin, S.B.H. Kent, J.P. Tam, R.B. Merrifield, Quantitative monitoring of solid-phase peptide synthesis by the ninhydrin reaction, *Analytical Biochemistry*, **1981**, 117, 147-157.
69. P.D. Josephy, T. Eling, R.P. Mason, The horseradish peroxidise-catalyzed oxidation of 3,5,3',5'-tetramethylbenzidine, *The Journal of Biological Chemistry*, **1982**, *257*, 7, 3669-3675.
70. C. Thibault, V. LeBerre, C. Casimirus, E. Trévisiol, J. François, C. Vieu, Direct microcontact printing of oligonucleotides for biochip applications, *Journal of Nanobiotechnology*, **2005**, 3, 7-18.
71. U. Kuhlmann, H. Jantoljak, N. Pfänder, P. Bernier, C. Journet, C. Thomsen, Infrared active phonons in single-walled carbon nanotubes, *Chemical Physics Letters*, **1998**, 294, 237-240.
72. B.R. Azamian, J.J. Davis, K.S. Coleman, C.B. Bagshaw, M.L.H. Green, Bioelectrochemical single-walled carbon nanotubes, *Journal of the American Chemical Society*, **2002**, 124, 12664-12665.
73. M.T. Martínez, Y-C. Tseng, M. González, J. Bokor, Streptavidin as CNTs and DNA linker for the specific electronic and optic detection of DNA hybridization, *The Journal of Physical Chemistry C*. Submitted.